

## Comparative study of Ag growth on (111) Au and Cu substrates

Y. Borensztein, T. Lopez-Rios, and G. Vuye

*Laboratoire d'Optique des Solides, Université Pierre et Marie Curie, 4 place Jussieu, 75252 Paris Cédex 05, France*

(Received 27 July 1987)

The growth of Ag monolayers on (111) Cu and Au substrates has been studied by Auger-electron spectroscopy and surface reflectance spectroscopy. At room temperature, Ag diffuses into the Au substrates, but grows continuously with a well-defined interface on Cu. The interdiffusion of Ag and Au is stopped when cooling the sample. In this case, the first Ag monolayer in contact with the Au surface behaves like a Ag-Au alloy. On the other hand, when deposited onto Cu, the first Ag monolayer displays a narrow absorption band at 3 eV which is not present in bulk. It could be due to transitions from *d* states in the Ag monolayer, the shift being caused by the interaction with Cu. The electronic properties of thicker films gradually tend to those of bulk Ag.

### I. INTRODUCTION

The electronic properties of metallic monolayers have been the subject of numerous studies for several years. Most of the theoretical calculations deal with "self-supported" layers; only a few of them are concerned with the interaction between a metallic monolayer, especially of Cu, and a given substrate.<sup>1-6</sup> Nevertheless the experimental investigations are, for obvious practical reasons, only interested in such systems.<sup>7-20</sup> This introduces supplementary problems to be studied, especially the mode of growth of the superficial metallic film and the electronic interaction between the substrate and the adlayer.

The present paper deals with the growth of silver on copper and gold substrates. The interest of these systems, for the present purpose, is due to the fact that the Ag film grows continuously, monolayer after monolayer, on these substrates.<sup>19,21</sup> However, in the case of Ag on Au, a bulk interdiffusion between the two metals occurs at room temperature, and it was necessary to cool the sample at low temperature in order to avoid this diffusion. Hence it was possible to obtain continuous Ag films with a given number of monolayers (from a half to several), either on Cu or on Au.

The experimental technique used here for the investigation of the electronic properties of the monolayers is the surface reflectance spectroscopy (SRS), which has been widely used for the study of surface properties or of chemisorption.<sup>7,22-25</sup> On the contrary, very few SRS experiments have been performed for investigating the growth of metal thin films.<sup>12,15,20</sup>

In Sec. II the experimental methods, the preparation of the samples, and their characterization are presented. The mode of growth was followed by Auger-electron spectroscopy and the results are given in Sec. III. Section IV is devoted to the theoretical aspects of the SRS; the measured quantity, namely the differential reflectivity, is given as a function of the dielectric functions of the different media, following several theoretical models. Finally, Secs. V and VI are devoted to the optical experimental results and to their discussion, respectively.

### II. EXPERIMENTAL METHODS

The preparation of the samples and the experimental studies (apart from the ones involving electron microscopy) were performed in the same ultrahigh-vacuum chamber ( $10^{-10}$  mbar). The substrate samples were prepared by *in situ* evaporation of high purity metals (99.999%) from tungsten crucibles warmed by the Joule effect. The metal molecules were condensed on smooth glass plates maintained at room temperature (RT), at a rate of about 0.6 nm/s, in order to achieve a total thickness from 40 to 80 nm depending on the samples. The pressure did not exceed a few  $10^{-9}$  mbar during the metal deposition. The Au and Cu substrates obtained in this way were formed of crystallites a few ten to a few hundred nm large. Figure 1(a) presents a transmission electron micrograph, obtained with a Philips EM300 microscope at 100 kV of a typical Cu sample. It shows the microcrystallites of Cu, some of them being large with a few dislocations, the grain boundaries, etc. The very small white spots are due to oxide clusters which have grown when putting the sample in air before introduction in the electron microscope. Figure 1(b) shows the corresponding diffraction pattern. The [220] ring is clearly the more intense one, while the [200] and the [111] ones are weaker, contrary to the case of a powder diagram. This indicates that most of the crystallites have a preferential orientation with the [111] direction perpendicular to the surface of the slab, with a possible small misorientation of a few degrees. It cannot be excluded that some of the crystallites display a [100] orientation. Nevertheless, it can be concluded that the surface is mainly a polycrystalline (111) surface. Electron microscopy experiments obtained on the gold substrates show similar results.

The Ag overlayers were deposited in the same way as the substrates. The Cu substrates were maintained at RT during Ag deposition, while the Au ones were either cooled to a low temperature of  $-150^{\circ}\text{C}$  (LT), or kept at RT. The rate of Ag deposition was 0.01 nm/s, and the pressure was maintained in the low  $10^{-10}$  mbar range. The amount of Ag atoms condensed on the substrates

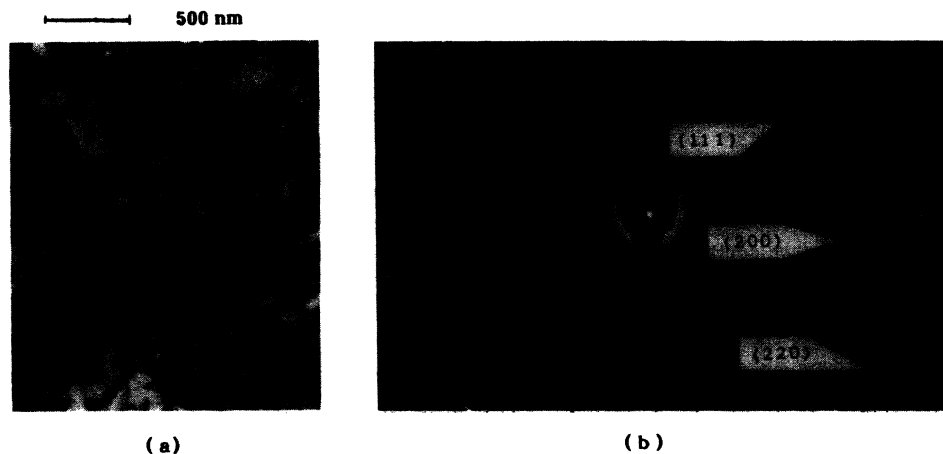


FIG. 1. (a) A transmission electron micrograph of a Cu film 60 nm thick. (b) The corresponding electron diffraction pattern.

was monitored by means of a 5 MHz oscillating quartz microbalance, calibrated beforehand by film-thickness measurements using x-ray interference in grazing incidence reflection.<sup>26</sup> The mode of growth for Ag on Cu was followed by Auger experiments performed with a four-grid Auger spectrometer.

The SRS technique consists of the measurement of the relative change of reflectance or differential reflectivity (DR) upon Ag adsorption:  $\Delta R/R = (R' - R)/R$ , where  $R$  and  $R'$  are the reflectances of the bare surface (Au or Cu) and of the same surface covered by Ag atoms, respectively. The optical spectrometer is schematized in Fig. 2. A monochromatic beam (1.4–5.2 eV), produced either by an uv Xe lamp or by a visible Wibbon one, is obtained by using a monochromator with two different gratings

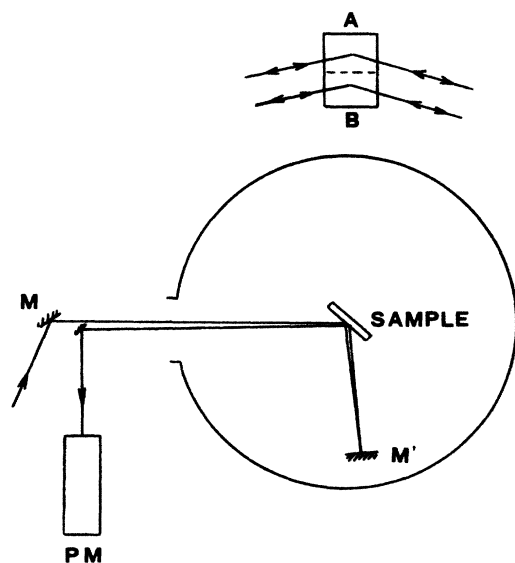


FIG. 2. The principle of the differential reflectometer. The light beam alternately impinges the two parts of the sample, perpendicularly to the figure plane, as indicated in the inset.

corresponding to the lamps. A polarizer determines the polarization of the light.

The beam impinges alternatively, by means of a vibrating mirror ( $M$ ), two halves of the sample: the first one ( $A$ ) is the substrate and is kept clean during the entire optical experiment by use of a shutter located in front of it when evaporating Ag; the other one ( $B$ ) is the Ag-covered surface. After a double reflection on the sample by use of a mirror  $M'$  inside the UHV chamber, the beam is focused on a photomultiplier (PM). A lock-in amplifier detection at the frequency of vibration of the vibrating mirror (800 Hz), combined with a feedback on the high voltage of the PM maintaining a constant value of the delivered current, provides a signal proportional to  $\Delta R^2/R^2 = [(R')^2 - R^2]/R^2$  (the beams are reflected twice on the sample). A simple calculation leads to a quantity proportional to the DR:  $\Delta R/R$ . A calibration operation is therefore needed in order to get the absolute values of  $\Delta R/R$ . The whole calibration procedure is described in Ref. 27, where other technical details can also be found.

### III. MODE OF GROWTH

The mode of growth of Ag on Cu was studied by Auger-electron spectroscopy. Figure 3 gives the variation of the peak-to-peak intensities of Auger peaks of Ag and Cu at 351–357 eV and 58–60 eV, respectively, versus the mass thickness of Ag deposits. The breaks in slope, which are visible in both curves at about 0.23 and 0.46 nm, as well as their exponential shape, are indicative of a Frank-Van der Merwe growth, i.e., a continuous, layer-by-layer growth.<sup>28</sup> Silver and copper are not miscible, and interdiffusion occurs only at high temperature.<sup>29,30</sup> Indeed, the Auger measurements did not give evidence of any diffusion. One can therefore conclude that the silver films on copper are continuous and uniform with a well defined interface. Moreover, the diffraction patterns obtained from Ag-covered Cu substrates in electron microscopy experiments indicated a parallel epitaxial growth of Ag on Cu (111).<sup>31</sup>

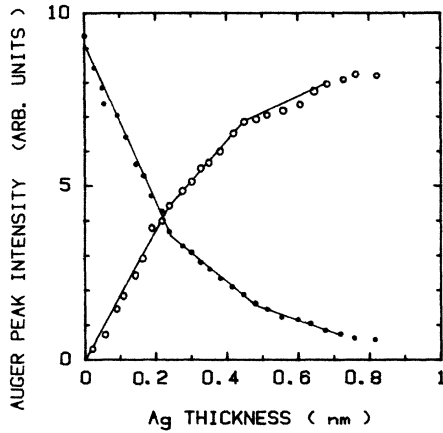


FIG. 3. The peak-to-peak intensity variation of the Auger peak of Cu (●) and of Ag (○) at 58–60 eV and 351–356 eV, respectively, vs the thickness of the Ag films. The intensities of the Ag peak were multiplied by 14.

Ag and Au, on the other hand, are essentially lattice matched. This results in the fact that the Ag film is in parallel epitaxy with the Au (111) substrate.<sup>32</sup> It has been demonstrated that at room temperature the growth of Ag on polycrystalline Au follows the layer-by-layer mode too.<sup>21</sup> However, Au and Ag are totally miscible, and a rapid interdiffusion occurs when the sample is warmed.<sup>33</sup> The interdiffusion already exists at room temperature but is then very much slower.<sup>33</sup> In this case, in spite of the epitaxial and layer-by-layer growth, the interface is not abrupt. In order to avoid the diffusion and to obtain a well-defined interface, as in the Ag/Cu case, it is necessary to cool the substrate. The optical results presented in Sec. V B display differences between the two kinds of growth at room or at low temperature.

#### IV. THEORY

##### A. The local three-phase model

In the usual theory of refraction, the different media, taken as homogeneous and isotropic, can be described by local and isotropic dielectric functions as indicated in Fig. 4.  $\epsilon^B(\omega)$  is the complex dielectric function of the bulk substrate,  $\epsilon^0(\omega)$  is that for the vacuum (which equals 1), and  $\epsilon^s(\omega)$  corresponds to the function for the surface region of thickness  $d$  which accounts for both the effect of the surface of the substrate and the presence of adsorbates. The Fresnel laws, derived from the Maxwell equations and continuity arguments, can be applied at the two interfaces. MacIntyre and Aspnes<sup>34</sup> have shown that when the thickness  $d$  is small with respect to the wavelength  $\lambda$  of the light, the reflectance of the system can be developed to the first order in  $d/\lambda$ . The differential reflectivity DR can therefore be written

$$\frac{\Delta R_s}{R_s} = \frac{R_s - R_s^0}{R_s^0} = \frac{8\pi d}{\lambda} \cos\theta \operatorname{Im} \left[ \frac{\epsilon^s - 1}{\epsilon^B - 1} \right], \quad (1)$$

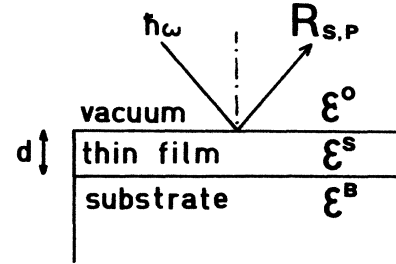


FIG. 4. A schematic diagram of the homogeneous multilayer model.

$$\begin{aligned} \frac{\Delta R_p}{R_p} &= \frac{R_p - R_p^0}{R_p^0} \\ &= \frac{8\pi d}{\lambda} \cos\theta \operatorname{Im} \left[ \frac{\epsilon^s - \epsilon^B}{\epsilon^B - 1} \frac{1 - (\epsilon^s - 1 + \epsilon^B - 1)\sin^2\theta}{1 - (\epsilon^B - 1 + 1)\sin^2\theta} \right], \end{aligned} \quad (2)$$

where  $\theta$  is the angle of incidence of the light and  $s$  and  $p$  refer to the polarizations of the light. In  $s$  polarization, the electric field is normal to the incidence plane (hence parallel to the surface), while in  $p$  polarization it is parallel to the incidence plane (hence with a nonzero component normal to the surface).  $R_s^0$  and  $R_p^0$  are the reflectances of the substrate without considering the surface-adsorbates region, and  $R_s$  and  $R_p$  the reflectances with the surface region. We can notice that the DR is proportional to the thickness  $d$  of the thin film, i.e., to the number of adatoms. The interesting quantity to study is, therefore,  $(1/d)\Delta R/R$ , the changes of which are directly related to the changes of the electronic properties of the adlayer, without any consideration on its thickness.

Within the MacIntyre and Aspnes (MA) model, the real and imaginary parts of the dielectric function  $\epsilon^s$  can be determined from two independent measurements, for example, in  $s$  and  $p$  polarizations, when the thickness  $d$  is known.  $\operatorname{Im}(\epsilon^s)$  is directly related to the optical absorption of the surface and adsorbed species: It therefore gives important physical information about the properties of the system under investigation.

##### B. Limitations of the three-phase model

Several authors have shown<sup>35</sup> that the usual local refraction model fails in explaining some aspects of the optical properties of surfaces. A long-wavelength electric field (of light, for example) can induce at a surface a short-wavelength response. In classical terms, it means that an induced charge exists at the surface or in the surface region. This problem occurs when the normal component of the electric field  $E$  is nonzero, i.e., in  $p$  polarization. In  $s$  polarization when  $E$  vanishes at the surface, no surface charge is induced and the usual theory of refraction, i.e., the MA model, gives a correct description of the surface optical properties. On the other hand, the hypothesis of local response leads in  $p$  polarization to two

unphysical consequences: The normal component of the electric field is discontinuous, and a density of charge is induced at the very surface. A microscopic theory of the dielectric response based on nonlocal relations between the response of the medium and the electric field acting on it is therefore needed to describe the optical response of the surface. Several microscopic theories have been developed for a jellium.<sup>36-38</sup> It has been shown that the response functions derived in that way are equivalent.<sup>39</sup> For example, Bagchi, Barrera, and Rajagopal<sup>38</sup> have introduced three response functions  $\delta\Lambda_x$ ,  $\delta\Lambda_y$ , and  $\delta\Lambda_z$ , defined by

$$\delta\Lambda_* = \int_{-\infty}^{+\infty} dz \left[ \int_{-\infty}^{+\infty} dz' \epsilon_{**}(z, z'; \omega) - \epsilon^{cl}(z; \omega) \right] \quad (3)$$

(for  $* = x, y$ ), where  $\epsilon^{cl}(z; \omega)$  is equal to  $\epsilon^B$  for  $z < 0$  and 1 for  $z > 0$  (see Fig. 5),

$$\delta\Lambda_z = \int_{-\infty}^{+\infty} dz \left[ \int_{-\infty}^{+\infty} dz' \epsilon_{zz}^{-1}(z, z'; \omega) - \epsilon^{cl}(z; \omega) \right], \quad (4)$$

$\delta\Lambda_*$  and  $\delta\Lambda_z$  can be interpreted as the surface/adsorbates excess in the averaged matrix dielectric function  $\epsilon_{**}(z, z'; \omega)$  and in the averaged matrix inverse dielectric function  $\epsilon_{zz}^{-1}(z, z'; \omega)$ , respectively. If we consider an uniaxial medium (it is the case here where the polycrystalline substrate is randomly oriented in the plane of the film), the two quantities  $\delta\Lambda_x$  and  $\delta\Lambda_y$  are equal. The differential reflectivities DR in *s* and *p* polarization can be expressed in this theoretical frame as a function of the two quantities  $\delta\Lambda_x$  and  $\delta\Lambda_z$ . The expressions of  $\Delta R/R$  are then identical to those obtained by Dignam, Moskovits, and Stobie<sup>39</sup> for a local but anisotropic medium, by introducing the components  $\epsilon_x$  and  $\epsilon_z$  of the surface dielectric tensor. This means that, for reflectance purposes, the surface response can be approximated by an effective local but anisotropic dielectric function. This shows that in *s* polarization, it is reasonable to apply the MA model by defining the surface dielectric function

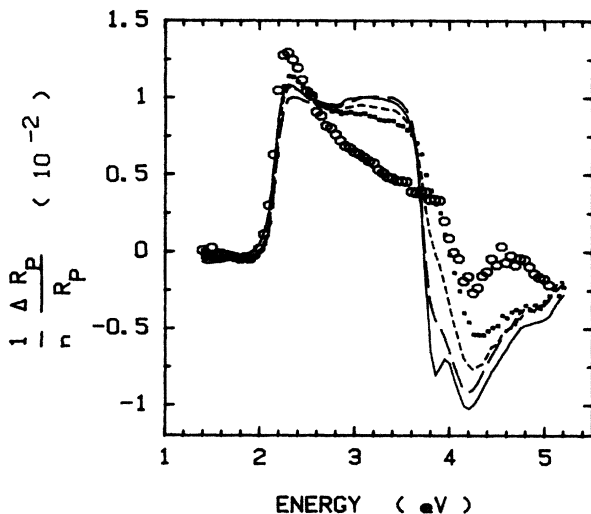


FIG. 5. Differential reflectivities (DR) spectra divided by the number  $n$  of Ag monolayers:  $(1/n)(\Delta R_p/R_p)$  for various deposits of Ag on the Cu substrate. The incidence of the *p*-polarized light was  $50^\circ$ .  $\circ$ , 1 ML;  $\cdots$ , 2 ML;  $---$ , 3 ML;  $---$ , 6 ML;  $---$ , 10 ML.

from Eq. (7), since  $R_s$  depends only on  $\delta\Lambda_x$ . On the other hand, the MA model is not adequate to describe the  $R_p$  quantity: For the MA model to be valid in *p* polarization, there ought to be an equality between the mean values of  $\epsilon_{xx}(z, z'; \omega)$  and of  $1/\epsilon_{zz}^{-1}(z, z'; \omega)$ . There is indeed no reason that these two quantities should be equal. Even if the surface region is isotropic, i.e., if  $\epsilon_{xx}$  is equal to  $\epsilon_{zz}$ , the mean values which appear in Eqs. (3) and (4) are generally different. This is due to the fact that, contrary to  $\delta\Lambda_x$ ,  $\delta\Lambda_z$  is the average of an inverse dielectric function. It is a good description of the response to a normal electric field, and its behavior is that of a loss function.

### C. A pragmatic standpoint

The previous paragraph has shown that the best description of the uniaxial system for its optical properties involves two complex quantities:  $\delta\Lambda_x$  and  $\delta\Lambda_z$ , or  $\epsilon_x$  and  $\epsilon_z$  which are the components of the effective surface dielectric function. Hence it involves four real quantities. Moreover, it is also necessary to know or to choose the thickness  $d$  of the region describing the surface and the adsorbates. However, it has been shown that it is not possible to perform four independent reflectance measurements in order to determine the four parameters, for example, one in *s* polarization at a given incidence and three in *p* polarization with different incidences.<sup>40</sup> One can try to get supplementary information from a Kramers-Kronig analysis of the reflectance spectra,<sup>41</sup> but this procedure is problematic because it requires an extrapolation of the measured reflectance to low and high frequencies. In the present case, such an extrapolation would lead to very uncertain results because the measurements are performed over a narrow spectral range. Since it was not possible in our case to apply the previously described microscopic model, we used the MA model in order to proceed further in the interpretation of the experimental results. By assuming an isotropic and local model and setting the thickness of the surface and adsorbate region, we were able to determine in several cases an effective local dielectric function  $\epsilon$  for the Ag thin overlayers on Au or on Cu. Once again, we remind that a dielectric function obtained in this way must be considered only as a crude approximation and has to be interpreted with much caution. However, it can give a better interpretation of the properties of the surface and the adsorbates than those which would be obtained directly from the reflectance spectra.

### D. The additive property of the differential reflectance in the MA model

Formulas (1) and (2) can be extended to the case where there are several thin films on the substrate, if the total thickness is much smaller than the wavelength of the light.<sup>42</sup> The expressions for the differential reflectivities are the sum of those corresponding to each different film considered as lying directly on the substrate:

$$\frac{\Delta R_s}{R_s} = \frac{8\pi \cos\theta}{\lambda} \sum_i d_i \operatorname{Im} \left[ \frac{\epsilon_i - 1}{\epsilon^B - 1} \right], \quad (5)$$

$$\frac{\Delta R_p}{R_p} = \frac{8\pi \cos\theta}{\lambda} \times \sum_i d_i \operatorname{Im} \left[ \frac{\epsilon_i - \epsilon^B}{\epsilon^B - 1} \frac{1 - (\epsilon_i^{-1} + \epsilon^{B-1}) \sin^2\theta}{1 - (\epsilon^{B-1} + 1) \sin^2\theta} \right], \quad (6)$$

$\epsilon_i$  and  $d_i$  are the complex dielectric function and the thickness of each film, respectively. It can be noticed that the order of the films is irrelevant: The optical responses of the layers are additive. An important consequence of this property will be used in this paper: It permits the determination of the individual optical contribution to the DR of the different monolayers (ML) of a thin film, notably of the superficial or the internal monolayers, by subtracting the spectra obtained for different numbers of monolayers deposited on the substrate. The validity of this procedure implies that the optical response of each layer is not too modified by the presence of the other layers. This hypothesis remains questionable, although it is correct in some cases, for example, when the electronic states are very localized on the atoms, as in the case of the  $d$  electrons in the noble metals which is our interest in this paper.

## V. OPTICAL RESULTS

### A. Silver on copper

All the experiments have been performed with  $s$ - and  $p$ -polarized light, in order to determine the effective adsorbate dielectric function. However, the curves obtained in the two different polarizations are rather similar, the intensities being only larger in  $p$  polarization, and the structures in the spectra more pronounced. So, we present here only the DR spectra measured with  $p$  polarized light. Figure 5 presents the DR spectra in  $p$  polarization divided by the mean thickness  $n$  [expressed in (111) Ag ML's] for various Ag overlayers on a Cu substrate:  $(1/n)(\Delta R_p/R_p)$ . The very narrow minimum at 3.8 eV, visible in the 10-ML spectrum, is due to an absorption caused by the excitation of a surface plasmon mode in the thin Ag film. We must note that this effect is peculiar to the  $p$ -polarization case and is not present in the  $s$ -polarization DR spectra. This mode, which corresponds to the coupling of the surface plasmons at the two interfaces of the Ag slab, is well known and is correctly reproduced by a classical calculation of the reflectance of a multilayer system.<sup>43</sup>

The disappearance of this negative peak for the thinner films can be explained by two phenomena: a size effect in the thin slab acting on the conduction electrons on the one hand, and the excitation by the  $p$  polarized light of longitudinal plasma waves (i.e., bulk plasmons) in the film, on the other hand. These two effects have been extensively studied in previous works.<sup>44-46</sup> Several features can be observed in all the spectra corresponding to

thicknesses larger than 1 ML, namely, a rapid increase of DR which becomes positive at 2.1 eV, then a decrease from about 3.9 eV. The shapes of these curves are explained by the fundamental optical properties of the noble metals. They correspond essentially to two kinds of electronic transitions: the intraband transitions, involving the  $s$ - $p$  conduction electrons (or "free" electrons), and the interband ones, involving mainly the  $d$ -band electrons (or "bound" electrons), which in this spectral range are transitions from  $d$ -band states to empty states above the Fermi level.<sup>47</sup> One can therefore separate the reflectance spectrum of a noble metal into two main regions. The first one is the free-electron region (I) from 0 eV up to the interband absorption edge (located at 2.1 eV in Cu and at 3.9 eV in Ag), where the reflectance is almost equal to 1. The second one is the bound-electron region (II), extending from the absorption edge to higher energies, where the reflectance is smaller.

The corresponding  $p$ -polarization reflectance spectra for the two metals were calculated and are given in Fig. 6, where the different regions are identified. When considering the system consisting of a thin Ag film on Cu, three regions can be defined: (1) 0–2.1 eV, intraband range for both metals, their reflectances are close to 1, and  $\Delta R/R$  is about 0; (2) 2.1–3.9 eV, intraband range for Ag and interband one for Cu,  $\Delta R/R$  is positive; (3) above 3.9 eV, interband range for both metals, the optical absorption in the Ag film is added to the Cu one, the reflectance of the sample is decreased, and  $\Delta R/R$  is negative.

These three regions are clearly separated in the experimental spectra of Fig. 5, except for the 1-ML spectrum where they are not so well defined. We can indeed observe that the shape of the 1-ML spectrum is different from the one for the thicker films. The 1-ML spectrum displays in particular a dip between 2.5 and 3.5 eV. A gradual change of the shapes of the different curves with the increase of the Ag film thickness is observed and is

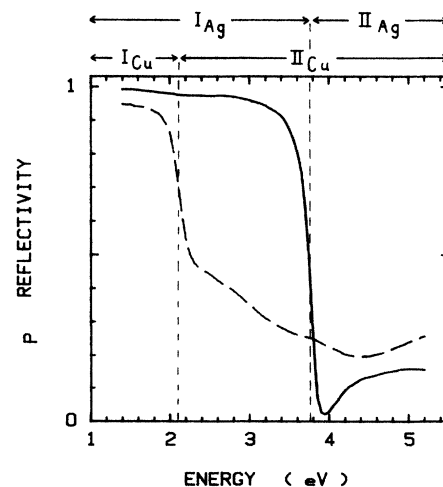


FIG. 6. Reflectivities of Ag and Cu substrates for  $p$ -polarized light at an angle of incidence of  $50^\circ$ . The intraband regions (I) and interband regions (II) are identified for both metals. —, Ag; --, Cu.

due to a weak remainder of this dip, disappearing for the thicker films. The additive property of DR (Sec. IV D) allows the separation of the contribution to DR of the first Ag ML from the Ag ML's deposited over this first one.

Figure 7 presents, besides the 1-ML spectrum, the spectra obtained with  $p$  polarized light corresponding to the additional layers, and given by

$$\left( \frac{1}{n-1} \right) \left[ \frac{\Delta R_p}{R_p}(n) - \frac{\Delta R_p}{R_p}(1) \right],$$

for  $n=2, 3$ , and  $6$ . These curves are almost identical over the entire spectral range. The main difference is the exact position of the DR decrease near  $4$  eV, which varies slightly in energy from about  $4.0$  eV for the thinner film to  $3.8$  eV for the thicker one. These spectra compare well enough above  $2$  eV with the theoretical curve calculated with bulk dielectric functions for silver and copper, which is also illustrated on the figure. The bulk dielectric function of silver has been taken from Ref. 48 with a decreased mean free path for the free electrons ( $2.5$  nm instead of  $40$  nm) in order to take into account the classical size effect in the thin film. The bulk dielectric function of Cu has been determined from absolute  $R_s$  and  $R_p$  measurements performed *in situ* on the substrate sample.<sup>27</sup> The similarity observed in Fig. 7 between the spectra corresponding to the Ag ML's above the first one emphasizes the specific optical and electronic behavior of the first-Ag monolayer, characterized by the dip in DR between  $2.5$  and  $3.5$  eV.

One can wonder whether this behavior is due to the fact that the first Ag ML is in contact with the Cu substrate or whether it is due to the fact that it is located at the free surface; in other words, whether the corresponding contribution to DR in a thicker Ag film is the one of the Ag ML close to the Cu substrate or the one of the

surface Ag ML. A comparison with the Ag/Au system in Sec. VI, for which no such behavior is observed, in spite of a similar mode of growth, will answer this question, showing that the effect is due to the contact with the substrate.

### B. Silver on gold

The electronic and optical properties of copper and gold are similar. The absorption edge of gold is located at  $2.45$  eV instead of  $2.1$  eV in copper and is not so abrupt.<sup>49</sup> In particular, it displays a relatively long "tail" below  $2.45$  eV. The main difference between the two systems Ag/Cu and Ag/Au lies in the fact that Ag and Au have almost identical lattice constants and that they are totally miscible.

It was shown in Sec. III that interdiffusion occurs at room temperature (RT). Two sets of experiments were, therefore, performed, one at RT, the other at a low temperature ( $-150^\circ\text{C}$ ) (LT) in order to limit the diffusion.

#### 1. Low-temperature experiments

For comparison with the Ag/Cu results, especially with Fig. 7, Fig. 8 presents the 1-ML spectrum and the contributions to DR of the various amounts of Ag deposited upon the first Ag ML, obtained by the difference

$$\left( \frac{1}{n-1} \right) \left[ \frac{\Delta R_p}{R_p}(n) - \frac{\Delta R_p}{R_p}(1) \right],$$

for  $n=2, 3$ , and  $5$ .

In this case too the last spectra are almost identical, the only difference being the decrease of DR at  $4$  eV. A theoretical spectrum obtained by calculation has also been illustrated on the figure. As previously, the Ag mean free path was reduced in order to take into account the size and defect effect in the thin Ag slab. In contrast to the Ag/Cu system, the experimental curves are not

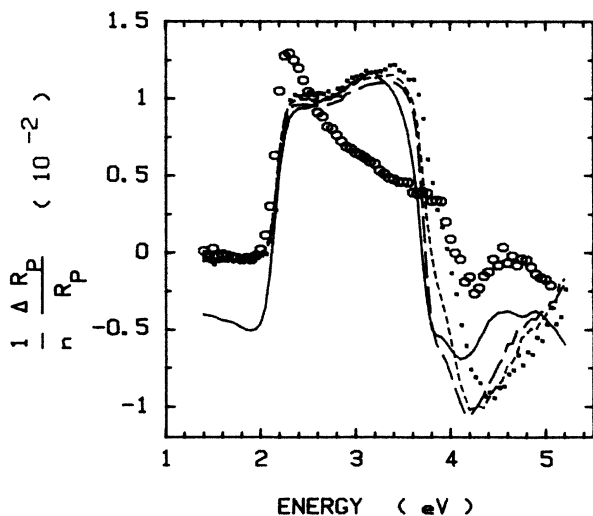


FIG. 7. DR spectra divided by the number  $n$  of Ag monolayers for various deposits of Ag above the first Ag monolayer on Cu, obtained by subtracting the 1-ML spectrum from the other ones.  $\cdots$ , (2-1) ML;  $---$ , (3-1) ML;  $---$ , (6-1) ML. The spectrum of the first Ag ML in contact with Cu is also drawn ( $\circ\circ$ ). The continuous line is a result of calculation.

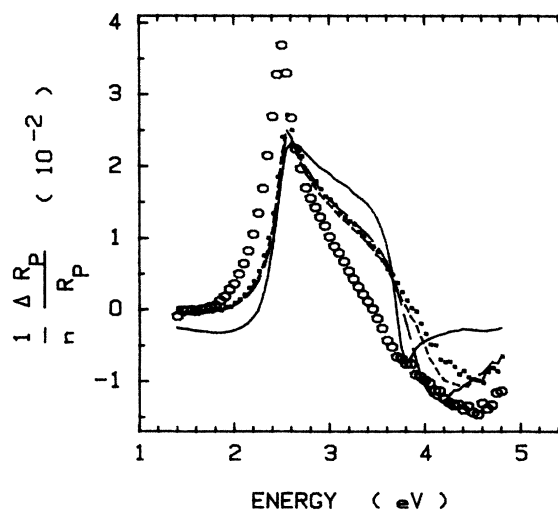


FIG. 8. DR spectra divided by the number  $n$  of Ag monolayers for various deposits of Ag above the first Ag monolayer on LT Au, obtained by subtracting the 1-ML spectrum from the other ones.  $\cdots$ , (2-1) ML;  $---$ , (3-1) ML;  $---$ , (5-1) ML. The spectrum of the first Ag ML in contact with LT Au is also drawn ( $\circ\circ$ ). The continuous line is a result of calculation.

very well reproduced. This may be due to the values used for the Au dielectric function which may not give correctly the optical reflectance of the Au substrate. However, calculations performed with dielectric functions from other references did not lead to a better agreement. The question remains, therefore, unanswered.

The 1-ML spectrum differs from the other ones by two main features: (1) the increase of reflectance above 2 eV starts at lower energy (by 0.1 or 0.2 eV) than for the following spectra, and (2) the general shape between 2.5 and 5 eV is smoother and without structure. The first point seems to be a surface effect from the gold sample, which is visible only when depositing the first Ag ML; it is probably related to the absorption tail below 2.4 eV observed in the experimental studies of the Au optical absorption.<sup>49</sup> It has been shown that the absorption edge in Au is split into two separate contributions: the onset of the *L* transitions at 2.45 eV and the onset of the *X* transitions at 1.94 eV.<sup>50</sup> It is possible that the *X* transitions at the surface of gold are modified by the presence of the Ag atoms, leading to a decrease of the optical absorption above 1.94 eV; hence, to an increase of reflectance, which is indeed observed in the DR spectrum for 1 ML of Ag. As for the second point, the differences between the 1-ML spectrum and the other spectra are not as striking as in the Ag/Cu case. It is not possible here to evoke an additional dip like in the previous case. The difference seems to be that the main decrease of reflectance which is at about 3.8–4 eV for the other spectra occurs at lower energy, around 3 eV, for the 1 ML one.

## 2. Room-temperature experiments

It has been emphasized that in this case interdiffusion occurs between silver and gold. However, this phenomenon depends on the temperature of the substrate. Gruzza, Guglielmacci, and Gillet<sup>51</sup> have obtained for the diffusion coefficient *D* for silver in gold at 20°C the value  $10^{-19} \text{ cm}^2 \text{ s}^{-1}$ . This indicates that Ag atoms can migrate along a depth of about 1 nm in the Au sub-

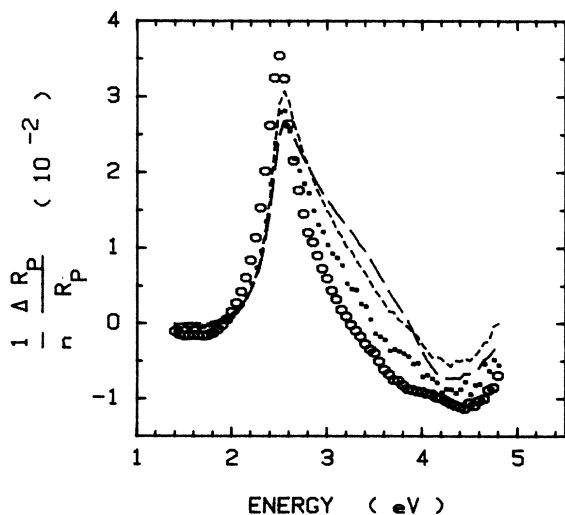


FIG. 9. Same as Fig. 8 for Ag deposited on RT Au. . . . , (1,5–1) ML; ---, (2–1) ML; —, (4–1) ML; ○○, first Ag ML deposited on RT Au.

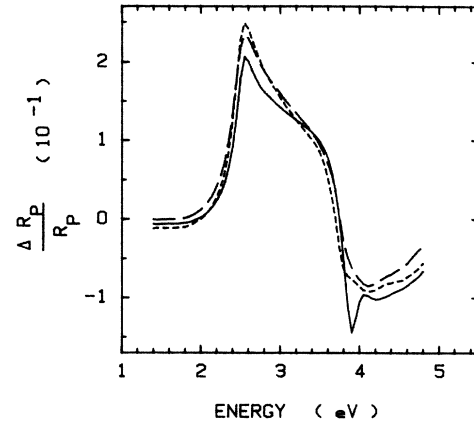


FIG. 10. DR spectra in *p*-polarized light for a 10-ML Ag film. —, deposited on the LT Au substrate; ---, deposited on the LT Au substrate after warming up to RT; -·-, deposited on the RT Au substrate.

strate at RT in a few hours only. In the experiments presented here, each spectrum was obtained in several tens of minutes: The Ag atoms could therefore migrate, but only a little, into the substrate. This means that, for small-Ag coverages, the interface between gold and silver must be diffuse with a varying silver concentration. This interdiffusion is indeed demonstrated by the optical measurements.

Figure 9 presents the DR spectrum measured with *p* polarized light for the 1-ML film and the spectra for the successive deposits obtained as before. Contrary to the low-temperature case illustrated by Fig. 8, there is a gradual change in the curves from the smallest coverage to the larger ones. The diffusion of silver in gold still occurs with thick films, leading to a diffuse interface between the two metals.

This diffuse interface is more clearly evidenced by the changes of the plasma resonance absorption in the Ag film at 3.8 eV. Figure 10 presents the DR spectra for a 10-ML Ag film deposited either on the LT substrate or on the RT one. In the first case, the resonance is sharp and intense, which indicates that the interface is abrupt and the plasmons at the interfaces well defined. In the second case, the resonance is not visible, which demonstrates that the interface is diffuse and the interface plasmon no longer defined. Moreover, when warming the first sample from LT up to RT, the resonance disappears too. The reflectance spectrum of this annealed sample, also given in Fig. 10, is almost identical to the one measured when silver was deposited directly on RT gold. The two systems, prepared in two different ways, are therefore identical with a diffuse interface.

## VI. DISCUSSION

### A. Silver on RT gold

The results obtained for Ag on Au at room temperature are easily explained by the formation of an alloy at the interface, and we shall not discuss them in detail. It

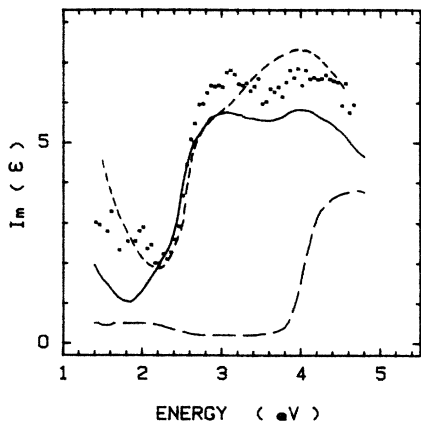


FIG. 11. Imaginary part of the effective dielectric function determined from DR measurements for a monolayer of Ag deposited on the RT Au substrate ( $\cdot \cdot \cdot$ ). The dielectric functions for bulk Ag ( $- -$ ) and bulk gold ( $-$ ) have been drawn (after Ref. 48), as also the dielectric function of a 21% Ag-Au alloy (after Ref. 52) ( $- \cdot -$ ).

is known that the electronic properties of Ag-Au alloys can be considered as intermediate between the Ag and Au ones. The  $d$  bands of Ag and of Au mix to form intermediate  $d$  bands, the energy location and shape of which depend on the relative proportion of each metal.

The behavior of this alloy is therefore similar to that of a noble metal with varying characteristics as a function of the concentration. For instance, the position of the absorption edge varies continuously from the bulk gold on to the bulk silver one.<sup>52</sup> The dielectric function of the 1-ML Ag film on RT gold substrate has tentatively been determined by using different thicknesses in order to model the alloy film of the corresponding concentrations, following the procedure explained in Sec. IV C. In all cases, the results are quite close to the dielectric function of bulk gold.

This is characteristic of a Au-Ag alloy with low concentration in Ag, as shown by Rivory.<sup>52</sup> As an example, Fig. 11 shows the so-determined imaginary part of the dielectric function, for an alloy thickness equal to 1 nm, in comparison with the ones of pure silver, pure gold, and Au<sub>79</sub>-Ag<sub>21</sub> alloy, after Ref. 52. This demonstrates clearly the hypothesis made in Sec. V B from kinetics arguments: At RT the silver atoms deposited on gold migrate into the substrate over a depth at least equal to 1 nm and form with Au a low-concentration alloy (of the order of 20% or even less). For a larger amount of Ag, no quantitative study can be attempted. The interface region is probably diffuse over a larger depth, with Ag concentration varying from a maximum value at the surface to a null one inside the sample. Moreover, the profile and the depth of the interface are dependent on the time elapsed between the Ag deposition and the optical measurements.

#### B. Silver on copper; silver on LT gold

Let us now consider the cases where Ag is deposited on cold gold and on copper. In both systems, no

interdiffusion occurs, and the growth follows the layer-by-layer mode. The two systems can therefore be compared. The effective dielectric function  $\epsilon$  has been calculated with the simple multilayer model from the experimental data for the 1-ML Ag film deposited either on Au or Cu, setting the thickness of the surface layer equal to the one for 1 Ag ML, namely 0.23 nm. Figures 12–14 present the real and imaginary parts of  $\epsilon$  compared with Ag bulk values.

In both cases the real part compares rather well with the bulk one and follows a Drude-like curve with negative values, characteristic of metallic properties. One can conclude that as soon as a 1-ML-thick film is deposited, the Ag film has a metallic character relatively close to the bulk one. This result is not surprising in view of the fact that the three metals under consideration are noble metals, for which each atom contributes in the same way to the conduction band, namely by giving one electron. Nevertheless, it is not possible from our results to obtain more information on the parameters describing the intraband transitions of the conduction electrons, because the contributions of the interband transitions in the 2–5-eV range, especially from  $d$  bands in the substrate as well in the Ag monolayer, are important. Results in the infrared range should be necessary to infer further conclusions.

In contrast, the imaginary parts, which are related to the optical absorption in the layer, are quite different for the two systems. For Ag on Cu (Fig. 13), the curve displays a narrow peak centered at about 3 eV but very small values above 4 eV, where larger values are present for bulk. This peak clearly corresponds to the dip observed between 2.5 and 3.5 eV in the 1-ML spectrum (Fig. 7), i.e., to an additional absorption. In contrast, when Ag lies on Au (Fig. 14), the curve has a broader peak around 4.3 eV and decreases slowly down to zero for lower energies.

The question which was asked in Sec. V A, namely whether the particular behavior of the first Ag ML on Cu

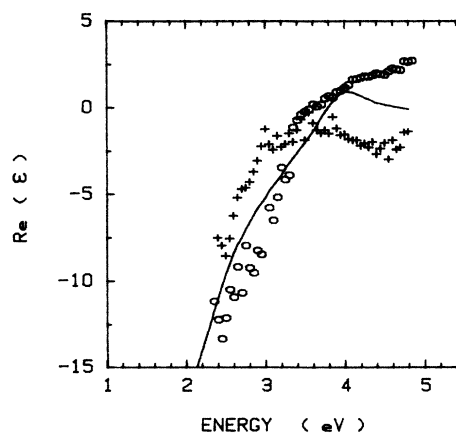


FIG. 12. Real part of the effective dielectric function determined from DR measurements for a monolayer of Ag deposited on the LT Au substrate ( $+$ ) and on the Cu substrate ( $o$ ). The dielectric function for bulk Ag ( $-$ ) has also been drawn (after Ref. 48).



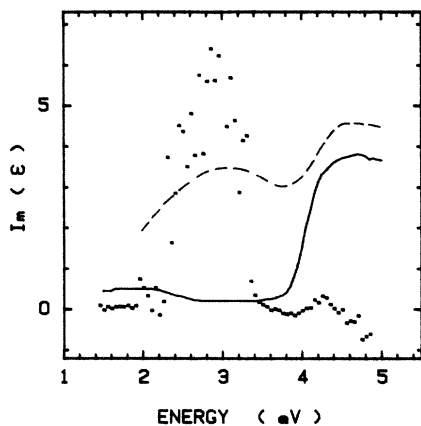


FIG. 13. Imaginary part of the effective dielectric function determined from DR measurements for a monolayer of Ag deposited on the Cu substrate ( $\cdot \cdot \cdot$ ). The dielectric function for bulk Ag (—), after Ref. 48, and for a 67% Ag-Cu alloy (---), after Ref. 53, have also been drawn.

is due to its superficial location or to the interaction with the substrate can now be answered. If it were due to the superficial character, the peak in  $\text{Im}(\epsilon)$  should be preeminent too in the Ag/Au system, which is not the case. Hence, this peak is a consequence of the interaction between Ag and Cu, whereas the interaction between Ag and Au is different. In this last case Ag on Au, the dielectric function compares quite well with the one obtained from optical measurements for a 62% Ag-Au alloy, which is also drawn on Fig. 14. It is clear from this agreement that the optical and electronic behavior of the Ag ML deposited on the LT Au substrate is the same as the one of a Ag-Au alloy with large concentration in Ag. The Ag ML is indeed in perfect epitaxy with the Au surface, which must lead to a large interaction between the

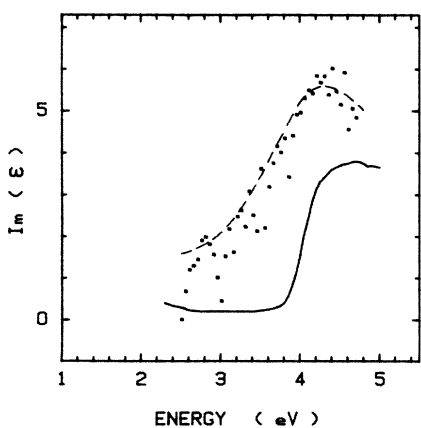


FIG. 14. Imaginary part of the effective dielectric function determined from DR measurements for a monolayer of Ag deposited on the LT Au substrate ( $\cdot \cdot \cdot$ ). The dielectric function for bulk Ag (—), after Ref. 48 and a 62% Ag-Au alloy (---), after Ref. 52, have also been drawn.

atoms of both noble metals in the same way as in a disordered alloy. Each Ag atom is indeed surrounded by 6 Ag atoms and 3 Au atoms, in almost the same proportion as in the 62% Ag-Au alloy.

The explanation for the Ag/Au system in terms of alloying cannot be applied to the Ag/Cu one. The result obtained for a metastable 67% Ag-Cu alloy, which has been drawn on Fig. 13 from Ref. 53, does not compare at all with the present result. The difference is that, contrary to the Ag/Au case, the Ag atoms deposited on Cu form a (111) ML mismatching the Cu surface. The interaction between Ag and Cu is therefore different and probably weaker than in the corresponding disordered alloy.

The imaginary part of the dielectric function for the Ag/Cu system has been determined as a function of the amount of Ag atoms and is presented in Fig. 15 for three coverages: 0.5, 1, and 2 ML. It gives a qualitative picture of the joint density of states, closely connected to the optical absorption in the layer. In bulk silver, the values of  $\text{Im}(\epsilon)$  above 3.8 eV correspond mainly to interband transitions from the  $d$  bands, but also to  $L_2 \rightarrow L_1$  transition located at the absorption edge. Photoemission experiments have shown that for very thin Ag films deposited on Cu (111) or Cu (100) (Refs. 9, 11, 13, and 14),  $d$  states exist with binding energies between 4 and 5 eV. For this reason, the relative small peak at 4.3 eV in the 2-ML spectrum can be interpreted as the convolution of  $d$  states located below 4 eV and empty states at or just above the Fermi level. On the other hand, the 0.5-ML spectrum does not display such a peak, and the 1-ML spectrum displays only a very weak one. It follows that this peak corresponds to the  $d$  states of the upper Ag layer of the 2-ML film and not to  $d$  states of the interfacial layer.

The appearance of the 4.3-eV peak, although strongly reduced in the 1-ML curve, is interpreted as due to the presence of Ag atoms upon the first Ag ML. It might

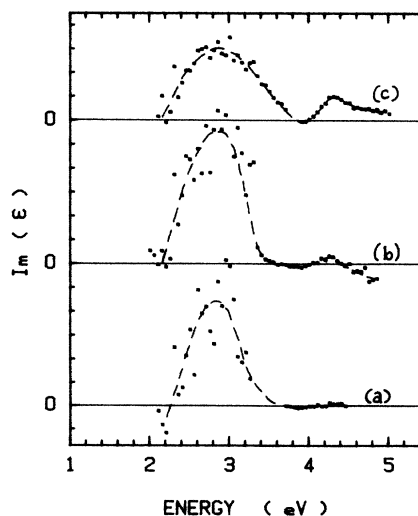


FIG. 15. Imaginary part of the effective dielectric functions determined from DR measurements for three different amounts of Ag deposited on Cu. (a) 0.5 ML, (b) 1 ML, (c) 2 ML.

occur that Ag does not follow a perfect Frank-Van der Merwe growth and that just before the first ML is complete, the second one begins to grow. Another explanation is the uncertainty in the determination of the mass thickness (about 5%) and the actual thickness may be a little larger than 1 ML. It must be noted however that the previous result for the 0.5-ML film is in contradistinction with the results of Ref. 14, where  $d$  states are observed between 4 and 5 eV. Except for this 4.3-eV peak, the spectra for 0.5 and 1 ML of Fig. 15 are almost identical. This similarity indicates that the 0.5 ML is composed of flat platelets 1 ML thick, covering half the sample, the optical and electronic properties of which are the same as the complete ML ones.

The peak observed in the curves just below 3 eV is clearly related to the additional absorption expressed in the DR spectra by a dip between 2.5 and 3.5 eV. Moreover, it is a specific effect of the first Ag ML. The determination of the effective dielectric constant  $\epsilon$  was attempted for the second ML of the 2-ML film from the spectrum obtained by differences as in Fig. 7, but values were found in the 2–3.6 eV range only, where no peak was indeed observed. The origin of this 3-eV peak is not clear, and we do not presently have a satisfactory explanation. Comparison with the photoemission experiments<sup>9,11,13,14</sup> cannot give any indication. The large density of states due to Cu between 2 and 4 eV prevents the observation of any feature due to the Ag atoms.<sup>13</sup> The spectra obtained in photoemission by the difference of the clean Cu surface spectrum from Ag-covered surface ones are not believed to give valid information in that energy range. Due to the small-escape length of photoelectrons (of the order of 1 nm or less), the presence of Ag atoms at the surface decreases the number of photoemitted electrons coming from the substrate. Hence, one cannot observe a possible feature due to photoelectrons emitted by the Ag atoms in the energy range of large density of states of the Cu substrate. In contrast, such an observation is possible with the SRS technique used here, because of the linearity of the DR for not too large amounts of adsorbed atoms, which means that the contribution to the reflectance due to the Cu substrate is not decreased by the presence of the Ag ad layer.

It is interesting to recall DR experiments performed by Beaglehole and Erlbach on Cu-Ag alloys.<sup>54</sup> They observed, for very low concentrations in Ag (<0.4%), DR spectra similar to our own for 1 ML and, for higher concentrations, spectra closer to the ones corresponding to thicker films. The explanation given about these different shapes was that in the former case the Ag atoms were isolated, while in the second one the charge distributions located around the Ag atoms interacted. However, in our system, the Auger experiments demonstrated without ambiguity the layer-by-layer growth. No interdiffusion occurs and there is no formation of a low-concentration alloy.

Another point to be noticed is that the 3-eV peak observed here is at the same energy as the  $d$  virtual bound state of Cu in Ag-Cu alloys with large concentration of Ag.<sup>55</sup> But in the alloy case the shape of  $\text{Im}(\epsilon)$  is very different to the one obtained here, as can be seen in Fig.

13. The alloying between the two metals, either with high or low concentration cannot be for these reasons, an explanation.

The fact that, especially for the 0.5-ML film, no peak is visible between 4 and 5 eV could lead one to think that there are  $d$  states at this energy in the first Ag ML and that the 3-eV peak could correspond to these  $d$  states, which would be at higher energies with respect to the Fermi level than in the bulk. However this argument requires an important static charge transfer from Cu to Ag in order to produce such a large shift of the  $d$  states. This is unlikely because of the equality of the electronegativities of the two metals. Moreover, if the 3-eV peak was due to electronic transitions from  $d$  states in the first Ag ML, one could expect a broadening and a gradual shift to larger energies, i.e., to bulk position of this peak when depositing the second Ag ML, which is not the case.

## VII. CONCLUSION

The growth of Ag on Cu and on Au was studied by SRS, a technique which has proved to be powerful for the study of the early growth. The optical properties of the two systems were compared. When deposited on RT Au, the Ag atoms diffuse in the substrate and form an alloy region with a continuously varying Ag concentration. For LT Au and RT Cu, the Ag film follows the Frank-Van der Merwe mode of growth. The additive property of the DR allowed an isolation of the optical response of the first Ag ML, even for thicker Ag films. It has been shown that for Ag on Au the Ag atoms of the first ML interact with the Au atoms of the substrate in the same way as in an equivalent alloy, leading to an absorption edge intermediate between the Ag and Au ones.

For Ag on Cu, the results are quite different. The absorption edge of Ag is observed only for the second ML, and it is then located close to the position in the bulk. For the first ML, a large optical absorption is instead observed at 3 eV, which corresponds to a peak at this energy in the imaginary part of the effective dielectric function of the Ag ML. An equivalent feature could not be seen in photoemission experiments because of the large density of states of the Cu substrate at 3 eV. Unfortunately, no convincing explanation is proposed here for the understanding of this new feature.

The interpretation in terms of Ag  $4d$  states shifted by 1 or 2 eV seems to be incorrect because of the unmatched growth which probably limits the interaction of the Ag  $d$  states with the Cu substrate and because of the important charge transfer needed to achieve such a shift, incompatible with the weak difference of the electronegativities of Ag and Cu.

## ACKNOWLEDGMENTS

We thank Professor J. Rivory for having provided unpublished results and for helpful discussions. We are grateful to Dr. M. L. Thève for her critical reading of the manuscript and to S. Fisson who took the electron micrograph pictures. The Laboratoire d'Optique des Solides is "Unité No. 781, associée au Centre National de la Recherche Scientifique," France.

- <sup>1</sup>B. R. Cooper, *J. Vac. Sci. Technol.* **10**, 713 (1973).
- <sup>2</sup>G. Cubiotti and B. Ginatempo, *J. Phys. F* **11**, 641 (1981).
- <sup>3</sup>P. J. Feibelman and D. R. Hamann, *Phys. Rev. B* **28**, 3092 (1983).
- <sup>4</sup>J. W. Davenport and M. Weinert, *Surf. Sci.* **144**, 220 (1984).
- <sup>5</sup>P. J. Feibelman and D. R. Hamann, *Phys. Rev. B* **31**, 1154 (1985).
- <sup>6</sup>J. E. Houston, C. H. F. Peden, P. J. Feibelman, and D. R. Hamann, *Phys. Rev. Lett.* **56**, 375 (1986).
- <sup>7</sup>J. Anderson, G. W. Rubloff, M. A. Passler, and P. J. Stiles, *Phys. Rev. B* **10**, 2401 (1974).
- <sup>8</sup>J. P. Biberian and G. A. Somorjai, *J. Vac. Sci. Technol.* **16**, 2073 (1979).
- <sup>9</sup>P. Heimann, H. Neddermeyer, and H. F. Roloff, in *Proceedings of the Seventh International Congress of Vacuum and the Third International Conference on Solid Surfaces*, edited by R. Dobrozemsky (Berger, Vienna, 1977), p. 2145.
- <sup>10</sup>P. Soukiassian, P. Riwan, and Y. Borensztein, *Solid State Commun.* **44**, 1375 (1982).
- <sup>11</sup>J. G. Tobin, S. W. Robey, L. E. Klebanoff, and D. A. Shirley, *Phys. Rev. B* **28**, 6169 (1983).
- <sup>12</sup>Y. Borensztein and G. Vuye, *Surf. Sci.* **162**, 991 (1985).
- <sup>13</sup>J. G. Tobin, S. W. Robey, and D. A. Shirley, *Phys. Rev. B* **33**, 2270 (1984).
- <sup>14</sup>A. P. Shapiro, A. L. Wachs, T. C. Hsieh, T. Miller, P. John, and T. C. Chiang, *Phys. Rev. B* **34**, 7425 (1986).
- <sup>15</sup>Y. Borensztein, *Surf. Sci.* **177**, 353 (1986).
- <sup>16</sup>B. Frick and K. Jacobi, *Surf. Sci.* **178**, 907 (1986).
- <sup>17</sup>V. Di Castro and G. Polzonetti, *Surf. Sci.* **186**, 383 (1987).
- <sup>18</sup>B. J. Knapp, J. C. Hansen, J. A. Benson, and J. G. Tobin, *Surf. Sci.* **188**, L675 (1987).
- <sup>19</sup>Y. Borensztein, *Europhys. Lett.* **4**, 723 (1987).
- <sup>20</sup>Y. Borensztein, T. Lopez-Rios, and G. Vuye, *J. Phys. F* **17**, 1093 (1987).
- <sup>21</sup>H. Tokutaka, K. Nishimori, and K. Takashima, *Surf. Sci.* **86**, 54 (1979).
- <sup>22</sup>G. B. Blanchet and P. J. Stiles, *Phys. Rev. B* **21**, 3273 (1980).
- <sup>23</sup>J. E. Cunningham, D. Gibbs, and C. P. Flynn, *Phys. Rev. B* **29**, 5304 (1984).
- <sup>24</sup>P. Chiaradia, A. Cricenti, S. Selci, and G. Chiarotti, *Phys. Rev. Lett.* **52**, 1145 (1984).
- <sup>25</sup>Y. Borensztein and F. Abelès, *Thin Solid Films* **125**, 129 (1985).
- <sup>26</sup>H. Kiessig, *Ann. Phys. (Leipzig)* **10**, 769 (1931).
- <sup>27</sup>T. Lopez-Rios, Y. Borensztein, and G. Vuye, *Phys. Rev. B* **30**, 659 (1984).
- <sup>28</sup>D. C. Jackson, T. E. Gallon, and A. Chambers, *Surf. Sci.* **36**, 381 (1973).
- <sup>29</sup>M. Murakami and D. de Fontaine, *J. Appl. Phys.* **47**, 2857 (1976).
- <sup>30</sup>G. Di Giacomo, P. Peressini, and R. Rutledge, *J. Appl. Phys.* **34**, 1626 (1974).
- <sup>31</sup>Y. Borensztein, Thèse de Doctorat d'Etat, Paris, 1985.
- <sup>32</sup>A. P. Shapiro, A. L. Wachs, T. C. Hsieh, T. Miller, P. John, and T. C. Chiang, *Phys. Rev. B* **34**, 7425 (1986).
- <sup>33</sup>A. Wagendristel, *Phys. Status Solidi A* **13**, 131 (1975).
- <sup>34</sup>J. D. E. McIntyre and D. Aspnes, *Surf. Sci.* **24**, 417 (1971).
- <sup>35</sup>See, for example, the exhaustive review by P. J. Feibelman, *Prog. Surf. Sci.* **12**, 287 (1982), and references herein.
- <sup>36</sup>K. L. Kliewer and R. Fuchs, *Phys. Rev.* **172**, 607 (1968); **185**, 905 (1969).
- <sup>37</sup>W. Plieth, H. Bruckner, and H. J. Hensel, *Surf. Sci.* **101**, 261 (1980).
- <sup>38</sup>A. Bagchi, R. G. Barrera, and A. K. Rajagopal, *Phys. Rev. B* **20**, 4824 (1979).
- <sup>39</sup>M. J. Dignam, M. Moskovits, and R. W. Stobie, *Trans. Faraday Soc.* **67**, 3306 (1971).
- <sup>40</sup>W. J. Plieth, *Isr. J. Chem.* **18**, 105 (1979).
- <sup>41</sup>R. E. Prange, H. D. Drew, and J. B. Restorff, *J. Phys. C* **10**, 5083 (1977).
- <sup>42</sup>J. D. E. McIntyre, in *Optical Properties of Solids. New Developments*, edited by B. O. Seraphin (North-Holland, Amsterdam, 1976), p. 555.
- <sup>43</sup>F. Abelès, in *Advanced Optical Techniques*, edited by Van Heel (North-Holland, Amsterdam, 1967), p. 143.
- <sup>44</sup>T. Lopez-Rios, M. De Crescenzi, and Y. Borensztein, *Solid State Commun.* **30**, 755 (1979).
- <sup>45</sup>F. Abelès, Y. Borensztein, M. De Crescenzi, and T. Lopez-Rios, *Surf. Sci.* **101**, 123 (1980).
- <sup>46</sup>Y. Borensztein, *J. Opt. Soc. Am.* **73**, 80 (1983).
- <sup>47</sup>H. Ehrenreich and H. R. Philipp, *Phys. Rev.* **128**, 1622 (1962).
- <sup>48</sup>P. B. Johnson and R. W. Christy, *Phys. Rev. B* **6**, 4370 (1972).
- <sup>49</sup>M. L. Thèye, *Phys. Rev. B* **2**, 3060 (1970).
- <sup>50</sup>M. Guerrisi, R. Rosei, and P. Winsemius, *Phys. Rev. B* **12**, 557 (1975).
- <sup>51</sup>B. Gruzza, J. M. Guglielmacci, and E. Gillet, *Thin Solid Films* **52**, 103 (1978).
- <sup>52</sup>J. Rivory, *Phys. Rev.* **15**, 3119 (1977).
- <sup>53</sup>J. Rivory (private communication).
- <sup>54</sup>D. Beaglehole and E. Erlbach, *Phys. Rev. B* **6**, 1209 (1972).
- <sup>55</sup>J. Rivory and M.-L. Thèye, *J. Phys. (Paris) Lett.* **36**, L129 (1975).

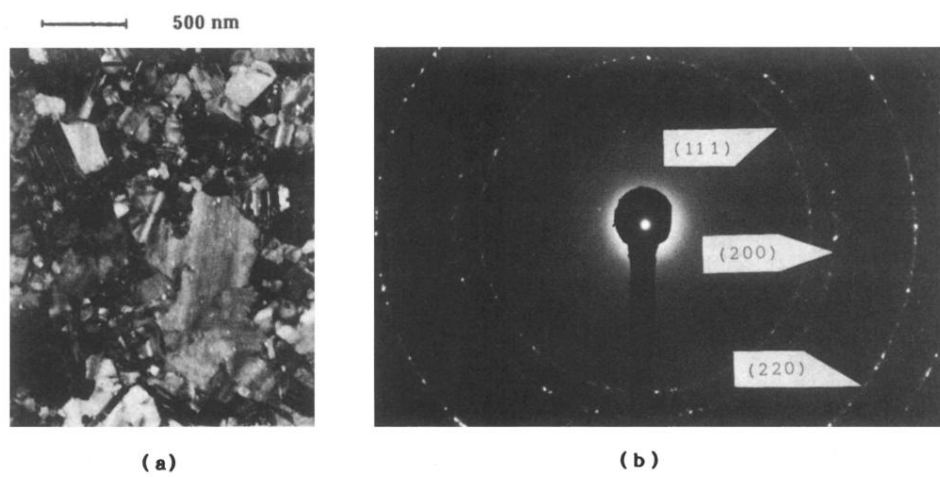


FIG. 1. (a) A transmission electron micrograph of a Cu film 60 nm thick. (b) The corresponding electron diffraction pattern.